ELSEVIER

Nanomedicine: Nanotechnology, Biology, and Medicine
46 (2022) 102611

nanomedicine
Nanotechnology, Biology, and Medicine

nanomedjournal.com

Ultrastable shelled PFC nanobubbles: A platform for ultrasound-assisted diagnostics, and therapy

Patrizia Nadia Hanieh, PhD[a,1], Caterina Ricci, PhD[b,1], Andrea Bettucci, PhD[c], Roberto Marotta, PhD[d], Carmel Mary Moran, PhD[e], Laura Cantù, PhD[b], Maria Carafa, PhD[a], Federica Rinaldi, PhD[a,*], Elena Del Favero, PhD[b,*], Carlotta Marianecci, PhD[a]

[a]*Department of Drug Chemistry and Technology, Sapienza University of Rome, Piazzale A. Moro 5, 00185 Rome, Italy*
[b]*Department of Medical Biotechnologies and Translational Medicine, University of Milan, Via Fratelli Cervi 93, 20090 Segrate, Italy*
[c]*Department of Basic and Applied Sciences for Engineering, Sapienza University of Rome, Via A. Scarpa 16, 00185 Rome, Italy*
[d]*Italian Institute of Technology, Via Morego 30, 16163 Genova, Italy*
[e]*Medical Physics, Centre for Cardiovascular Science, University of Edinburgh, 47 Little France Crescent, EH16 4TJ Edinburgh, United Kingdom*

Revised 6 September 2022

Abstract

Nanoscale echogenic bubbles (NBs), can be used as a theranostic platform for the localized delivery of encapsulated drugs. However, the generation of NBs is challenging, because they have lifetimes as short as milliseconds in solution. The aim of this work has been the optimization of a preparation method for the generation of stable NBs, characterized by measuring: a) acoustic efficiency, b) nano-size, to ensure passive tumour targeting, c) stability during storage and after injection and d) ability to entrap drugs. NBs are monodisperse and ultrastable, their stability achieved by generation of an amphiphilic multilamellar shell able to efficiently retain the PFC gas. The NBs perform as good acoustic enhancers over a wide frequency range and out of resonant conditions, as tested in both *in vitro* and *in vivo* experiments, proving to be a potential platform for the production of versatile carriers to be used in ultrasound-assisted diagnostic, therapeutic and theranostic applications.

Keywords: Nanobubbles; Ultrasound contrast agents; Acoustics; Theranostics; Drug delivery

Introduction

Microbubbles, comprising a gas core and stabilizing outer shell, have been used in diagnostic US imaging as contrast agents (UCA) since the early 1990s after it was demonstrated that an outer shell extended the bubble lifetime *in vivo*.[1] The enhancement of the ultrasound signal is a result of the acoustic impedance mismatch between the microbubbles and the surrounding medium. Recently, the potential role of such microbubbles as theranostic drug delivery systems has also been the focus of much research.[2]

At present, the UCAs approved for clinical use by FDA are relatively few: Optison (GE Healthcare Inc., Princeton, NJ, USA) and Definity (or Luminity, Lantheus Medical Imaging, Inc. N. Billerica, MA, USA), enclosing perfluoropropane (C_3F_8); and Lumason (or SonoVue, Bracco Imaging SpA, Milan, Italy) enclosing sulfur hexafluoride (SF_6).[3] Sonazoid, enclosing perfluorobutane (C_4F_{10}), is used in Asia and Norway for liver and breast imaging.[4]

Due to their size (1–5 μm), MBs cannot extravasate from intravascular into interstitial space. Consequently, in a clinical setting, the US contrast agents are used to qualitatively assess vascular perfusion defects and, by their dynamic enhancement, to provide differential diagnosis of organ abnormalities.[5] On the other hand, pilot work has shown that by functionalization of the MBs shell, MBs may have the potential to differentiate between malignant and benign tumors[6] and there has been increasing

* Corresponding authors.
E-mail addresses: patrizianadia.hanieh@uniroma1.it (P.N. Hanieh), caterina.ricci@unimi.it (C. Ricci), andrea.bettucci@uniroma1.it (A. Bettucci), roberto.marotta@iit.it (R. Marotta), carmel.moran@ed.ac.uk (C.M. Moran), laura.cantu@unimi.it (L. Cantù), maria.carafa@uniroma1.it (M. Carafa), federica.rinaldi@uniroma1.it (F. Rinaldi), elena.delfavero@unimi.it (E. Del Favero), carlotta.marianecci@uniroma1.it (C. Marianecci).
[1] These authors contributed equally.

https://doi.org/10.1016/j.nano.2022.102611
1549-9634/

interest in the potential of MBs as integrated systems for theranostic applications, with drugs encapsulated within the microbubble structure.[7] Real-time monitoring of the bubbles could be achieved by non-destructive US detection, and subsequent drug release could be triggered by higher-pressure US, with localized therapeutic impact. Preclinical *in vivo* studies incorporating chemotherapeutics have shown encouraging results while lowering the impact of adverse effects.[8–10] Nonetheless, the size of MBs remains one of the major limitations, as tumour targeting requires crossing the permeable tumour vessel walls, with vascular endothelial gaps in the size-range of hundreds of nanometers.

Nano-sized bubbles (NBs) can potentially overcome this impasse as they can extravasate and enter tumour tissue.[11] Once there, NBs could accumulate *via* the enhanced permeability and retention effect,[12] promoting efficient uptake either directly or by drug-release stimulated by an US field. However, this promising application poses additional constraints to the design of bubble systems with appropriate structure and *in vivo* high performance.

The generation of NBs is challenging, and indeed whether NBs can exist is a source of controversy in the literature. Nano-sized bubbles are considered significantly more unstable than micro-sized bubbles, and their lifetime can be as short as milliseconds before they dissolve into the solution.[13] The use of hydrophobic gases, such as C_3F_8 or SF_6, is expected to slow down the gas leakage from NBs,[14] further improving the bubble longevity with heavier perfluorocarbons (PFCs), such as C_4F_{10}, C_5F_{12}, and C_6F_{14}. However, the high boiling temperature of these PFCs and the NBs-associated Laplace pressure, may lead to the formation of nanodroplets, with liquid- rather than gas-core, at physiological temperature. Indeed, several studies describe a strategy, based on the formulation of nanodroplets, with a liquid core undergoing a liquid-to-vapour transition when exposed *in situ* to an intense acoustic pulse (acoustic droplet vaporization).[15,16] Nanodroplets can extravasate into interstitial spaces before activation, while the "activated" bubbles can be used for both diagnostics and drug delivery. However, there are limitations to this technology — until they are activated, nanodroplets cannot be visualized by US imaging; significant acoustic pressures are required to initiate droplet vaporization; and bubbles formed *in situ* by acoustic vaporization, tend not to be in the sub-micron range, but rather micro-bubbles.

The possibility to generate stable NBs for theranostic application is therefore a topic of great interest. Several studies suggest that long-lived nano-sized bubbles can exist,[13,17,18] although whether the 'bubbles' are gas-filled, nanodroplets or nanoparticles continues to be a challenging issue.[19]

The proposed protocols to produce lipid-shell NBs are similar to those employed for MBs production. A key factor in the manufacture and stability of NBs is the presence of an interfacial shell,[20] where phospholipids, proteins, or polymers may help in reducing the interfacial tension, extending the life of nanobubbles.[21] Precise shell engineering can improve nanobubble stability and provide a level of resilience to mechanical deformations induced by ultrasound insonation or during circulation.[18] The selection of the composition and formation of the interfacial envelope, together with the choice of enclosed gas, is of importance to obtain diagnostically and therapeutically useful NBs.[22,23]

The aim of this paper is to describe the design and construction of a NBs platform for both drug delivery and echogenic signal enhancement. NBs were prepared and characterized exhaustively with respect to the following key-enabling properties: a) acoustic efficiency, b) nano-size, to ensure passive tumour targeting, c) stability during storage and after tail vein injection and d) ability to entrap lipophilic and hydrophilic drugs. Two types of NBs were manufactured using this platform — innovative surfactant NBs and phospholipid-based NBs. Both types of nanobubbles were filled with PFC gas, that is biocompatible, inert, and chemically highly stable and is not metabolized in the body after injection.[24]

The physical-chemical characterization of the systems was performed by combining complementary experimental techniques. Static and Dynamic Light Scattering (SLS, DLS), fluorescence spectroscopy, shelf-life and biological stability studies, combined with Small-Angle X-ray Scattering (SAXS) and cryo-electron (CryoEM) tomography experiments, were used to unravel the multilayer structure of the NBs, to test their resistance to stress and deformation and to determine their stability during their notably extended shelf-life. Acoustic measurements *in vitro* and in a pilot *in vivo* study demonstrated acoustic enhancement of the nanobubbles compared to a commercial microbubble product.

Methods

1,2-Dimyristoyl-sn-glycero-3-phosphocholine (DMPC) was from Avanti Polar Lipids (Alabaster, Alabama, USA). Dicetyl phosphate (DCP), Sorbitan monolaurate (Span20), cholesterol (Chol), Hepes salt {*N*-(2-idroxyethyl) piperazine-*N*′-(2-ethanesulfonicacid)}, pyrene, diphenylhexatriene (DPH), calcein, Nile Red, human serum (HS), bovine serum (BS), tetradecafluorohexane (PFC) were from Sigma-Aldrich (Milan, Italy). Sonovue® was generously gifted by Bracco (Milan, Italy).

Phospholipid-based or surfactant-based vesicles were prepared by thin-film hydration method. Details in the Supplementary Material.

Experimental techniques

Structural characterization

Static and dynamic laser light scattering (SLS), ζ-potential and density measurements were performed on samples at 25 °C.

Cryo Transmission Electron Microscopy (Cryo-TEM) and cryo-electron tomography images were acquired on frozen hydrated samples of NBs using a Tecnai G2 F20 microscope (FEI company, the Netherlands). Computation of tomograms and postprocessing were performed using the IMOD 4.9.2 software package.[25]

Small Angle X-Ray Scattering (SAXS) measurements were performed at the ID02 high-brilliance beamline at the ESRF Synchrotron (Grenoble, France). From the SAXS intensity spectra, information on the size, shape and internal structure of the particles in solution could be obtained. Data fitting was

performed with the SaSView application (version 4.2.0, 2019)[26] with a core multi-shell spherical model.

Bilayer fluidity of NBs was evaluated by using the hydrophobic probe 1,6-diphenyl-1,3,5-hexatriene (DPH).[27] In parallel, bilayer polarity and microviscosity were determined by fluorescence experiments on NBs loaded with Pyrene, used to detect the lateral distribution and mobility of the enveloping membrane compounds.

Experimental details in the Supplementary Material.

Pulse-echo and photoacoustic analysis

In order to test the shelf stability of the NBs, a pulse-echo technique was used to determine the acoustic behavior of the NBs at different concentrations and time-points after preparation. The presence of the gas inside NBs was confirmed by the photoacoustic technique.[28] Details on the experiments in the Supplementary Material.

NBs stability and probe-loading studies

The time stability of NBs, stored at room temperature and T = 4 °C up to 90 days, and upon contact with human serum or bovine serum up to 45 % (over 3 h at T = 37 °C) was evaluated, by determining the average size and ζ-potential.

The presence of inner gas in the NBs was tested by acoustic attenuation measurements (after 90 days at 4 °C) and SAXS measurements (after 30 days at 4 °C).

In order to check the ability of NBs to entrap drugs and gas, simultaneously, fluorescent probes, namely, Calcein and Nile Red, as models for hydrophilic and hydrophobic molecules, respectively, were both included within the NBs during preparation. Loaded NBs were characterized in terms of acoustic efficiency, entrapment efficiency, size and ζ-potential in comparison to unloaded NBs.

Echographic studies

The small animal imaging studies were carried out in accordance with the UK Home Office Animals (Scientific Procedures) Act, 1986 and the European Committees Council Directive of November 1986 (86/609/EEC) and were assessed by the University of Edinburgh Ethical Review Committee. Details on the experiment are reported in the Supplementary Material.

Results and discussion

Preparation of NBs

As the first and crucial step,[17,29,30] we focused on the protocol for the production of stable NBs. The optimization of the NBs fabrication protocol constitutes the first result of this work. A set of experimental techniques were applied to assess that the preparation procedure led to the effective formation of NBs upon internalization of the gas into closed amphiphilic shells, hereafter called vesicles, either phospholipid- or surfactant-based.

NBs were prepared by using different phospholipids and surfactants, together with cholesterol (Chol), in different molar ratio. The sonication parameters and the technique of gas supply were the critical factors in the formation of the NBs.

Liquid PFC was added with a syringe to a vesicular dispersion, at room temperature, and submitted to sonication for 15 min, with an ultrasound generator equipped with a microprobe operating at 20 kHz, with amplitude of 16 % (Vibracell-VCX 400-Sonics, USA). During sonication, temperature increased to 70 °C. Then the nanobubbles dispersion was cooled by thermal shock in melting ice, for 10 min. Care was taken to avoid PFC loss by sealing the container. As a final step, the NBs were purified at 25 °C by centrifugation in a MPW-260R (MPW Med. Instruments) at 600 rpm for 20 min.

Finally, the low-HLB Span20 surfactant and the phospholipid DMPC, also in association with the anionic surfactant DCP, were chosen as the most effective constituents in the formation of NBs (Table S1). DMPC is generally used to prepare liposomes due to its good biodegradability, biocompatibility, low immunological responses, and similarity with the cell membrane structures.[31] As an alternative component, the non-ionic surfactant Span 20 is advantageous due to its resistance to oxidation, chemical stability, low cost, and ease of packaging and storing conditions.[32,33] Compared to the phospholipid-based liposomes, niosomes composed of Span are able to form multi-layered vesicles useful to deliver both hydrophilic and lipophilic drugs.[34] Furthermore, several researchers have shown the possibility to functionalize both these compounds to deliver vesicles to a specific target.

The final gas volume concentration was derived by calculating the mean internal volume of the bubbles at a given surfactant concentration. The external size of the bubbles and the thickness of their shell were obtained from DLS and SAXS results. Given the polydispersity in bubbles size and shell thickness, an indicative estimate of the gas concentrations in the final suspensions gives about 20 mm^3/ml for phospholipid-based NBs and 6 mm^3/ml for surfactant-based NBs, which is comparable to the commercial SonoVue (Bracco) formulation (8 mm^3/ml, as stated by the manufacturer).

General suitability of NBs

NBs were submitted to a range of experimental tests to verify their structural and acoustic properties.

The populations of NBs were quite monodisperse (PDI ≤ 0.2) with 150–175 nm mean size (Table 1). The ζ-potential ranged from weakly negative for DMPC-based NBs to markedly negative for Span20-based NBs (−42 ± 2 mV). The addition of 24.7 mM of the anionic surfactant DCP conferred a higher negative ζ-potential (−71 ± 2 mV).

The crucial test was to verify the presence of a gas core inside the NBs, which was performed by density, static light scattering (SLS) and acoustic analysis.

The density of NBs suspensions was measured in the temperature range 20–70 °C and compared with the density of the corresponding vesicles at the same lipid and surfactant concentration (Supplementary Material, Table S2). At 20 °C, the density of vesicles and NBs suspensions is higher than that of the solvent. This is due to the density of amphiphiles (and higher for Span20) and in the case of NBs suggests the possible

Table 1
Size (DLS), charge (ζ-potential) and bilayer characterization in terms of fluidity (anisotropy measurements) and polarity and microviscosity (pyrene fluorescence spectra evaluation) of different NBs. Listed values are determined as the mean ± standard deviation of n = 3 NBs sample measurements.

Sample	Size (nm) ± SD	ζ-Potential (mV) ± SD	PDI	Fluidity (anisotropy)	Polarity (I_1/I_3)	Microviscosity (I_E/I_3)
DMPC NBs	151 ± 3	−4 ± 1	0.20	0.25	1.05	0.44
DMPC-DCP NBs	130 ± 2	−71 ± 2	0.20	0.24	1.07	0.43
Span20 NBs	173 ± 4	−42 ± 2	0.12	0.24	0.95	0.3

coexistence in the core of perfluorohexane in the gas phase (density about 0.01 g/cm^3) and in the liquid phase (density 1.7 g/cm^3). Interestingly, the temperature dependence of the density is clearly different for systems with or without PFC, as reported in Fig. 1.

Although the absolute values of the density for the DMPC-based and Span20-based systems depend on the lipid/surfactant type and concentration, the volume of the internal cage and thickness of the shell, the hallmark of the gas presence can be observed.

The density of the DMPC-based vesicles suspension decreases slightly as temperature is raised. Reversely and notably, the density of the DMPC-based NBs dispersion hugely decreases and between 30 °C and 40 °C it is already lower than the solvent water. This result stems from the presence of gas in the NBs at physiological temperatures, well below the boiling point of Perfluorohexane (bp = 56.6 °C).

For the Span20-based systems, while the density of the vesicle solution slightly declines as temperature is raised, that of NBs steeply drops at temperatures higher than 50 °C, as reported in Fig. 1 Panel B.

To further test the presence of gas in NBs at physiological temperatures, below 40 °C, all suspensions were submitted to external mechanical compression, directly in the cell of the density meter ($\Delta p = 2 \times 10^5$ N/m^2), and then, once compression had been released, their density was measured again. The density of vesicle suspensions is not affected by compression, as expected for an amphiphilic shell enclosing an incompressible aqueous core. Conversely, the density of the NBs suspensions is dramatically altered after compression, both in absolute values and in the temperature dependence, becoming similar to the parent vesicles (Panels A and B, Fig. 1). This finding suggests that the increase of external pressure disturbed the NBs shells inducing their shrinkage and then the leakage of the gas.

Moreover, vesicles and NBs were observed by SLS at T = 25 °C. The intensity scattered from NBs is 10-fold the one from the corresponding vesicles at the same concentration (Supplementary Material, Table S3). This significant difference cannot

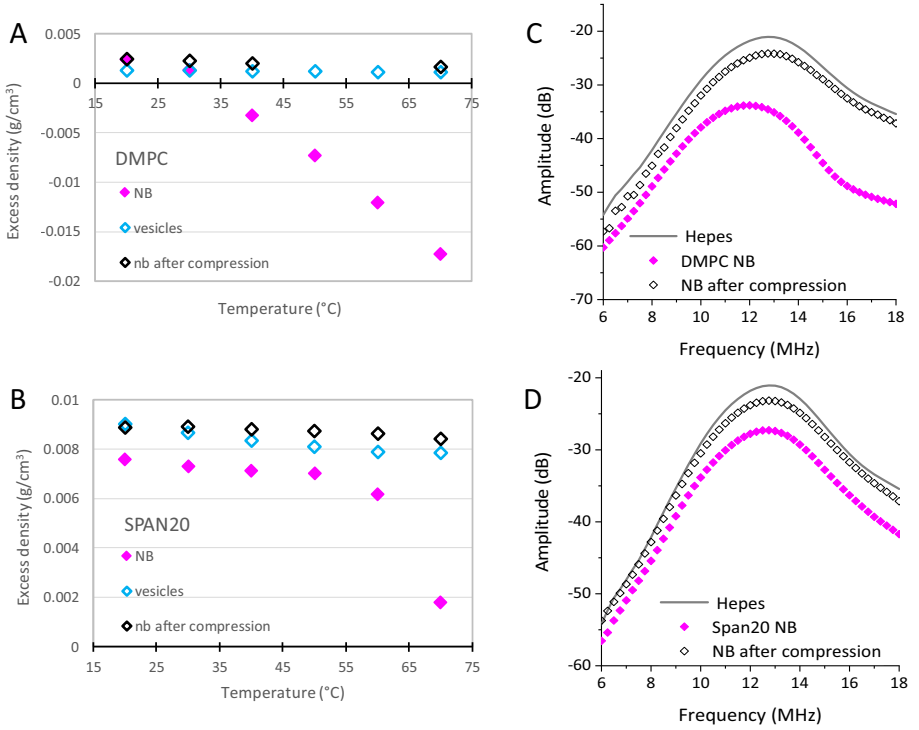

Fig. 1. Excess density of samples with respect to water at different temperatures, Panel A DMPC, Panel B Span20. Amplitude of the ultrasound signal after traversing the test-cell over the frequency range 6–18 MHz, DMPC Panel C, Span20 Panel D. The amplitude of the ultrasound signal measured for the solvent (Hepes) is reported for comparison.

be attributed only to the 20 % different size, but rather depends on a higher contrast of NBs (see Methods section), suggesting that gas-PFC is enclosed in NBs even at 25 °C.

In parallel, the acoustic efficiency of NBs was measured by a pulse-echo technique before and after mechanical compression ($\Delta p = 2 \times 10^5$ N/m^2).

Results (Fig. 1, Panel C and Panel D) clearly show that the considerable efficiency of both DMPC-based and Span20-based NBs in attenuating the US beam vanishes after compression, becoming similar to that of the buffer.

The presented set of results, obtained with complementary techniques, confirms the actual presence of gas-phase-PFC inside the NBs, also in the 25–40 °C temperature range. Inside the NBs, the gas-PFC is probably in equilibrium with a small volume of liquid-PFC and is trapped and stabilized by a closed shell built by the amphiphilic molecules, which is capable of withstanding the overpressure of curvature without collapsing.

Acoustic efficiency

The acoustic efficiency of the NBs was evaluated with a pulse-echo technique and compared to one of SonoVue®. Fig. 2 shows the attenuation of the incident acoustic beam at 14 MHz for DMPC NBs, Span20 NBs and SonoVue® microbubbles systems, as a function of concentration, expressed as estimated gas concentration. The central frequency of the ultrasound transducer (14 MHz) is out of the resonance range for both the SonoVue® (about 2.5 MHz[35]) and NBs (higher than 20 MHz, see Fig. S1, Supplementary Material).

As expected, and reported in Fig. 2, acoustic attenuation increases almost linearly with concentration for both NBs preparations. The attenuation values are comparable for NBs and SonoVue® at similar estimated gas concentration. In addition, for Span20 NBs, the frequency spectra of the US signal attenuation, at different concentrations, are reported in Figs. S1 and S2, Supplementary Material, showing similar attenuation efficiency across the analyzed frequency range (6–20 MHz) both in Hepes buffer and in water.

The efficiency of gas trapping within the NBs was also evaluated using a photoacoustic cell and the results were compared with those obtained for SonoVue® (Fig. S3, Supplementary Material). Dampening of the vibration amplitudes for the first and second resonance frequencies of the photoacoustic cell confirm that NBs and SonoVue® are comparable for gas trapping and acoustic performance.

Morphology and internal structure of NBs

The morphology and the internal NBs structure can affect the volume of encapsulated gas and their stability both in *in vitro* and *in vivo* conditions. A detailed investigation of the morphology and structure of the NBs was performed by Cryo-EM, SAXS and fluorescence analyses.

CryoEM projection images and cryo electron tomographies revealed that all samples contain subspherical nanobubbles with a characteristic electron-transparent gas-enriched core (see Fig. 3). In DMPC-based NBs, most particles have a multi-lamellar envelope, but some nanoparticles are unilamellar (see Fig. 3, top row, A–C). Some electron-dense diffuse material, probably liquefied gas, is present between the membrane and the gaseous core in many nanoparticles (see Fig. 3B–C). The morphology of DMPC-DPC-based nanoparticles is not significantly different (see Fig. 3, central row, D–F). Conversely, the Span20 NBs sample contains nanoparticles with distinctive and different morphology. A thick and massive shell surrounds the electron transparent core, suggesting that the envelope is likely to have a multi-lamellar structure (see Fig. 3, bottom row, H–J). Also in this system, some irregular electron-dense material, again probably liquefied gas, is visible inside the core itself. Finally, in all samples we observed several nanoparticles devoid of gas and many vesicles, that could either be present in the formulations or partially emptied during rapid freezing.

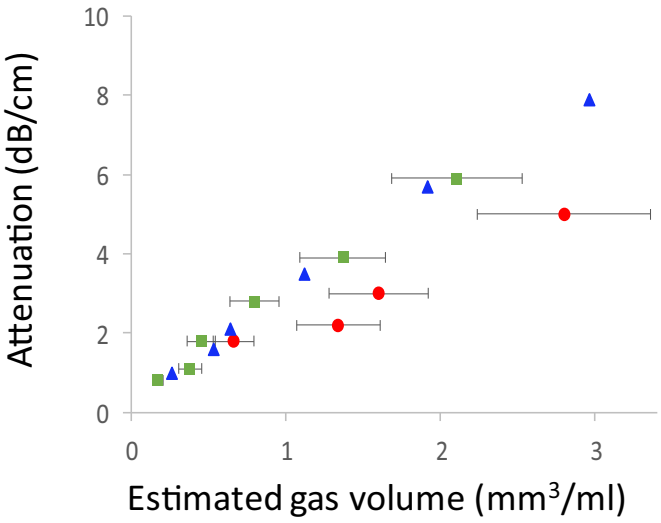

Fig. 2. Acoustic attenuation at 14 MHz for Span20 NBs (green squares), DMPC NBs (red dots) and SonoVue MBs (blue triangles) in Hepes buffer at different estimated gas concentrations vol/vol (error bar ±20 %, for SonoVue the gas content is stated by manufacturer).

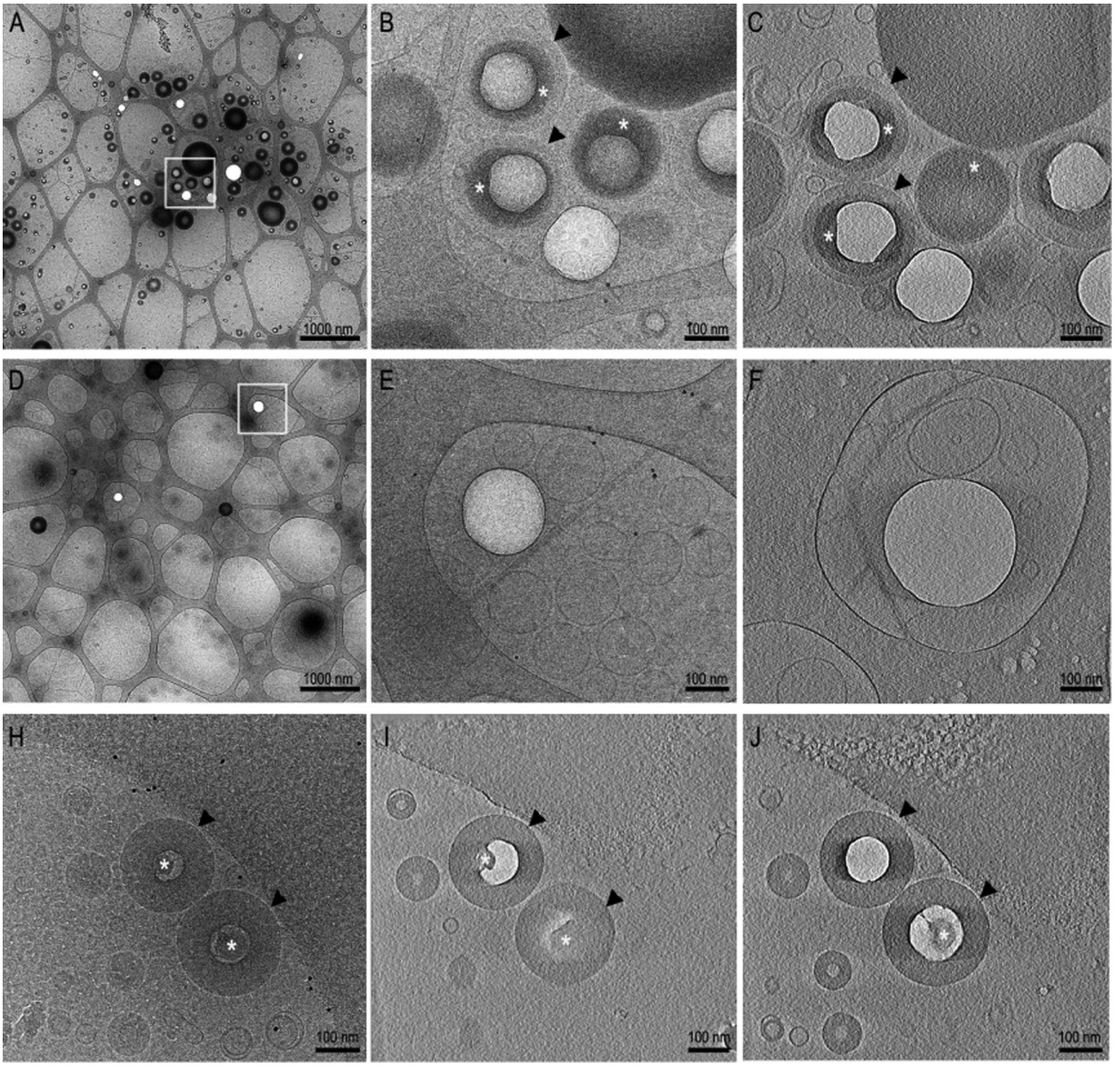

Fig. 3. Cryo-EM and cryo-tomography. Top row, DMPC-based NBs: A) low magnification projection image of vitrified sample; B) higher magnification of the region boxed in A; C) tomographic slice (10 averaged sections) showing DMPC NBs. Central row, DMPC-DPC-based NBs: D) low magnification projection image of vitrified sample; E) higher magnification of the region boxed in D; F) tomographic slice (10 averaged sections) showing DMPC-DPC NBs. Bottom row, Span 20-based NBs: H) high magnification of particles; I) and J) are different tomographic slices (10 averaged sections) showing Span20 NBs. Black arrowheads and white asterisks point respectively to multi-lamellar membranes and electron-dense regions.

The structure of the various NBs was assessed by SAXS. The analysis of the intensity spectra measured for NBs, reported in Fig. 4, reveals interesting structural features and confirms the presence of a gas core.

For ease of discussion, we report the intensity profile of DMPC-DCP NBs together with that of DMPC-DCP vesicles (Fig. 4B). Differences are clearly visible in the $q < 1\ nm^{-1}$ region, revealing primary features of the overall particles. The scattered intensity at low-q is orders of magnitude higher for DMPC-DCP NBs than for vesicles. This result confirms the presence of gas inside the NBs, as the scattered intensity is proportional to the square of the difference in electron density between the particles, and in particular of their gas core and the solvent. Also, the intensity decay is much steeper for NBs. The straight black line drawn on top of the experimental spectrum follows a decay behavior of $I(q) \div q^{-4}$, which is characteristic of hard interfaces between two physical media.[36] This reveals that the interface between the gas core and the surrounding stabilizing DMPC-DCP shell is well defined, as expected for gas bubbles in water. Similar comparison is shown for all NBs in Fig. S4, Supplementary Material, and the same observations are applicable for all the investigated systems. Deviation from the q^{-4} decay below $q = 0.05\ nm^{-1}$ indicates that the size of the nanobubbles is of the order of hundreds of nanometers, in agreement with DLS results.

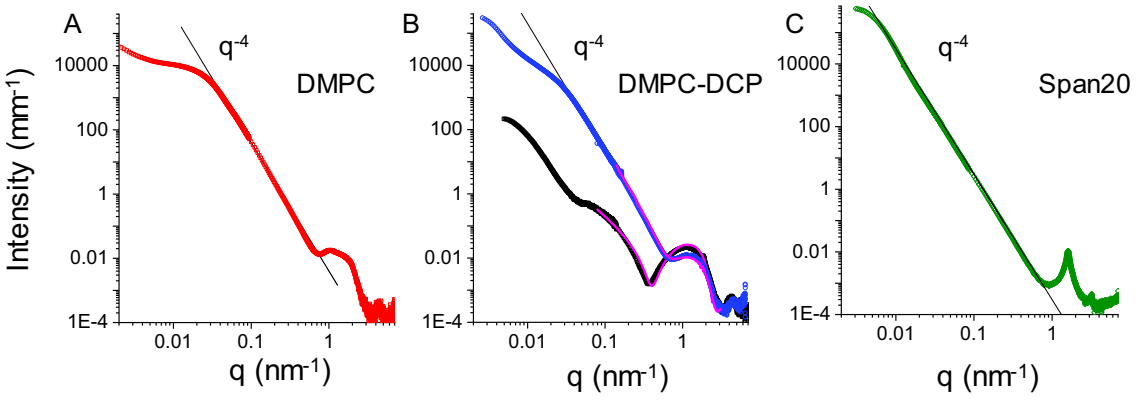

Fig. 4. SAXS intensity spectra for different NBs. A) DMPC (red), B) DMPC-DCP (blue), C) Span20 (green). Straight black lines draw the decay behavior I(q) ÷ q^{-4}, characteristic of hard interfaces between two physical media. The spectrum of a simple water-enclosing DMPC-DCP closed bilayer (black) is also shown in panel B for comparison with the corresponding gas-enclosing DMPC-DCP NBs, together with the bilayer fits (magenta).

On the local length-scale, the structure of NBs is reflected in the features of the intensity spectra at $q > 0.1$ nm^{-1}. An identical form factor of a single closed lipid bilayer, about 5 nm thick, has been used to model both the external shell of DMPC-DCP vesicles and of NBs. In the NBs an inner gas core replaces the water core of vesicles (electron density profiles are reported in Fig. S5, Supplementary Material). We suggest that an additional lipid monolayer is present at the PFC-water interface, allowing for the stabilization of the gas-in-liquid nanobubble. The enclosing lipid lamellar shell can constitute a good barrier against PFC diffusion.

DMPC NBs display a local structure very similar to that of DMPC-DCP NBs, particles being enclosed by a bilayer of lipids. A fraction of multilamellar shells is present, as inferred by the small characteristic peak around 1 nm^{-1}. The formation of multilamellar shells is expected for lipids with low charge.

Span20 NBs gives rise to quite a different intensity spectrum, shown in Fig. 4D. Bragg peaks at $q = 1.6$ nm^{-1} and 3.2 nm^{-1} emerge, corresponding to a characteristic repeat distance inside the particle of 3.8 nm, interestingly, roughly twice the length of a Span20 molecule. Exactly the same structure peaks are observed for the Span20 vesicles (see Fig. S4, Supplementary Material) as already reported.[37] In the Span20 NBs the gas core is surrounded by a multilayered shell made of stacked adjacent bilayers without interlamellar water, thus detailing the CryoTEM observation of a thick and massive shell.

The presence of unilamellar or multilamellar enveloping shells can be a key parameter both for the stability of the NBs and for the efficiency in the encapsulation of both hydrophobic and hydrophilic drugs, in view of their use as drug delivery systems.

To evaluate the propensity of NBs to host and then release entrapped drugs, the NBs shell fluidity, polarity and microviscosity have been measured. Results show that NBs are equipped with bilayers with average values of fluidity, microviscosity and polarity, useful to entrap, retain and then release lipophilic drugs[38] (Table 1). The parent vesicles show identical values (Table S4, Supplementary Material) confirming the encapsulation of the gas totally in the inner compartment of NBs, without influencing bilayer features.

Stability of NBs

The NBs morphology, structure and physico-chemical properties are promising for the development of a commercial product to be used in diagnostics or theranostics. For this purpose, the Span20 NBs display the most favorable combination of features (small size, multi-layered shell), that have to be paralleled by good storage and biological stability.

Shelf-life stability of Span20 NBs was assessed checking particle size and surface charge over 3 months at two different storage temperatures, and SAXS profiles were also taken at 30 days' post-preparation. Parallel investigation was performed on DMPC NBs, for comparison. In Fig. 5, NBs behavior upon storage is presented.

NBs are stable with respect to size and charge up to 90 days at both storage temperatures. Also, their internal structure is preserved, as tested by SAXS measurements performed after 30 days. Span20 NBs are particularly stable, showing both the same internal structure and total volume fraction (Fig. 5, Panel D). Notably, NBs maintain their acoustic properties almost unchanged after 90 days' storage (Fig. 5, panels E and F).

Overall, the novel NBs presented here display outstanding stability (size and ζ-potential, persistence of acoustic signal and gas retention), significantly better than commercial products. For example, SonoVue® solution, prepared according to the manufacturer's specifications, was found to lose its acoustic properties in approximately 4 days, as evaluated by pulse-echo and photoacoustic measurements (Supplementary Material, Fig. S6).

As for the acoustic efficiency and biological stability of NBs, they have been tested at temperatures up to 40 °C (Fig. S7). In Fig. S8, Supplementary Material, data related to hydrodynamic diameter and ζ-potential before experiment and after contact with 45 % (v/v) human serum (time 0–3 h) are reported. NBs display good stability, at least 180 min. Stability

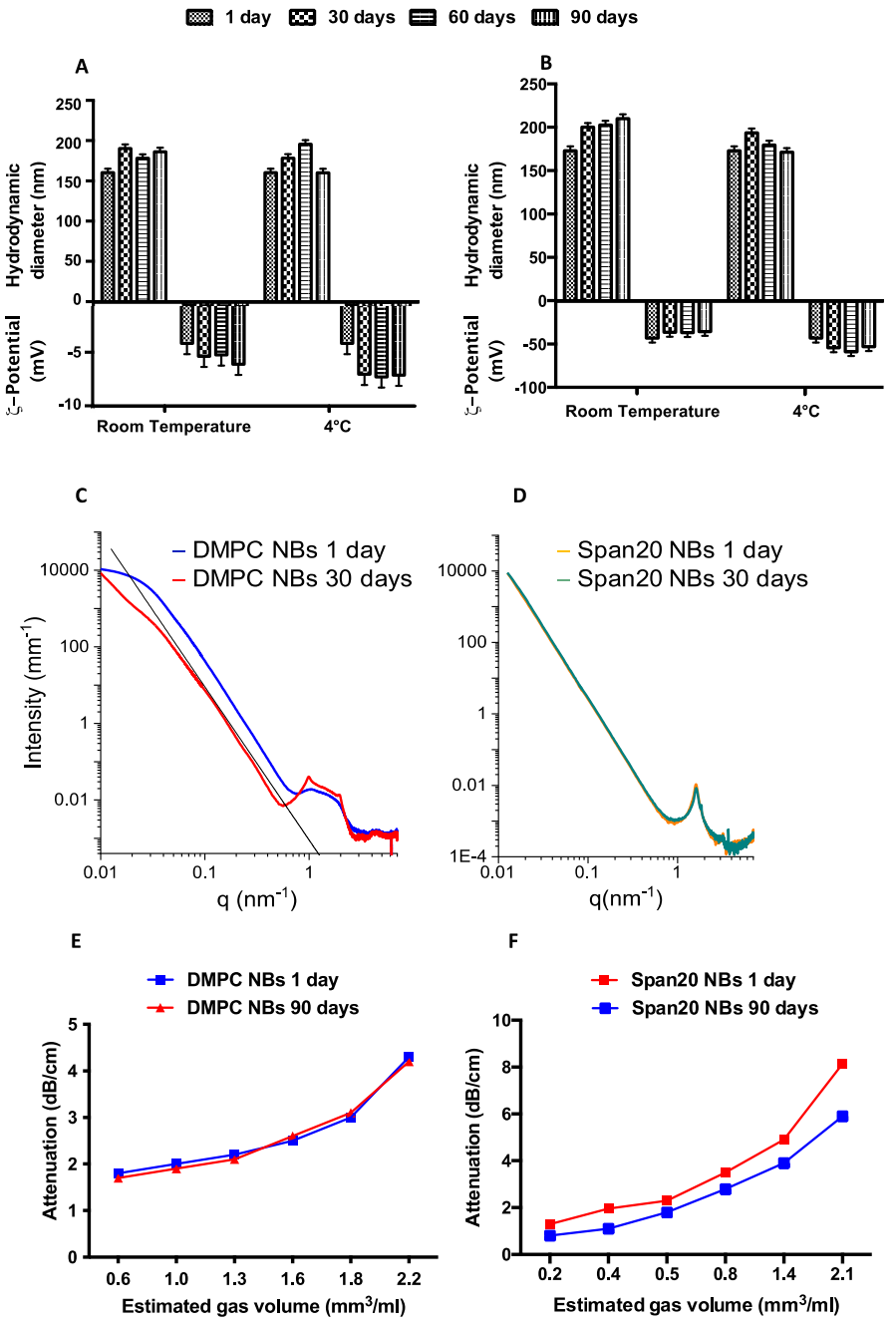

Fig. 5. Time stability of DMPC NBs (left column) and Span20 NBs (right column). A), B): Hydrodynamic diameter and ζ-potential, up to 90 days at two different storage temperatures (RT and 4 °C). C), D): Comparison of SAXS intensity spectra taken at preparation and after 30 days of storage. E), F): Ultrasonic (14 MHz) attenuation of NBs diluted in Hepes buffer at different estimated gas concentrations, at preparation and after 90 days of storage.

was tested also in bovine serum (Fig. S9, Supplementary Material) with similar results.

NBs as a putative theranostic platform: drug-gas co-loading and in vivo pilot-testing

The long time stability and persistence of the NBs even in serum emerges as a prominent property of the novel NBs presented here. In particular, Span20 NBs display the best performance in terms of size, stability, prolonged gas retention and acoustic properties. These features support their application as a multipurpose platform, both as new contrast media and as drug carriers, *via* the co-loading of gas and drugs, suitable for controlled release. To investigate the potential of NBs as a dual diagnostic and theranostic platform, Span20 NBs were submitted to further investigation to explore their potential for drug loading and *in vivo* use.

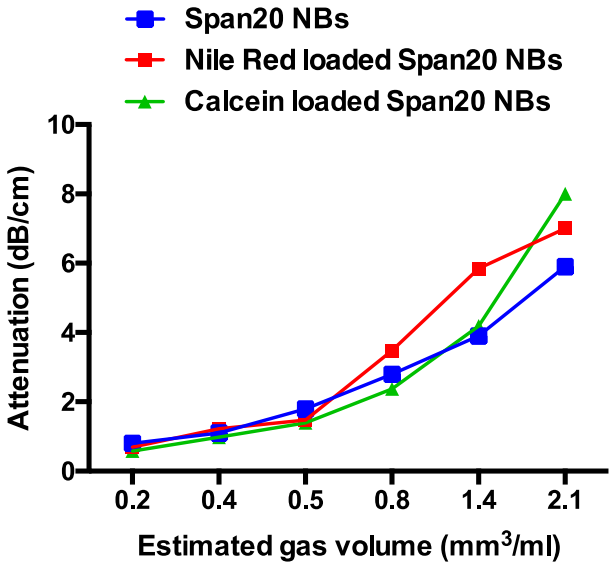

Fig. 6. Ultrasonic (14 MHz) attenuation of Span20 NBs, without (blue) and loaded with fluorescent probes (red and green), upon dilution in Hepes buffer at different estimated gas concentrations with respect to the prepared formulations.

Span20 NBs were loaded with two fluorescent probes, the hydrophilic calcein and the hydrophobic Nile Red, as mimics of small drugs. Their presence in Span20 NBs was checked by measuring their fluorescent signals (Table S5, Supplementary Material). Moreover, amplitude attenuation results reported in Fig. 6, show that the co-loading of gas and drug mimics maintains the acoustic efficiency of the NBs.

Notably, it appears that the thick multilayered envelope of Span20 NBs sustains their ability to efficiently solubilize both hydrophilic and hydrophobic drugs with relatively low impact on their stability and echogenicity. In fact, the peculiar tightly layered structure of Span20 NBs shell provides the opportunity to efficiently solubilize hydrophobic compounds in the lipophilic compartments of the stacked bilayers, while hydrophilic small drugs can be hosted in the alternating hydrophilic layers, together with hydrated headgroups of the surfactant. The release of model drugs is not prevented, and the Nile Red release profile can be observed within 24 h (Fig. S10).

Finally, given the outstanding performance of Span20 NBs, and in view of the development of an innovative theranostic platform, it was selected for a pilot test *in vivo* in a mouse model. After administration, a rapid sustained enhancement of echographic signal for over 60 s (as ethically allowed) was monitored within the mouse carotid artery (Fig. 7A and video in Supplementary Material) demonstrating the Span20 NBs utility as an ultrasonic contrast agent, with notable persistence. Images were acquired both at 30 MHz and at 40 MHz and demonstrated marked enhancement at both frequencies (Fig. 7B, C). Comparable enhancement is also observed for SonoVue® microbubbles in the 30–40 MHz frequency range, but previous experimental and modelling studies suggest that only a discrete sub-population of SonoVue® bubbles contribute to signal enhancement at these high frequencies,[3] likely requiring decantation of SonoVue® for signal optimization. Conversely, as shown in the preceding sections, Span20 NBs are smaller in size, and relatively mono-disperse, and their resonance frequency is much higher (>20 MHz, Fig. S1). The present *in vivo* pilot test, then, highlights the potential of Span20 NBs as a contrast agent for preclinical imaging studies and for small animal veterinary applications.

Conclusions

The proposed NBs formulations, prepared according to an easy and reproducible protocol, demonstrate physical and chemical properties suitable for it to be applied as a multipurpose agent for US-assisted applications. Detailed characterization and focused tests show that selected compounds for the interfacial envelope, both DMPC and especially Span 20 together with cholesterol are able to form NBs that display key structural features, namely, they are constituted by a monodisperse and ultra-stable population of shelled nano-sized bubbles, stabilized by an amphiphilic multilayered shell. Differently from nanodroplets, which have to be activated by an intense acoustic pulse (acoustic droplet vaporization) or by heating,[15,16] NBs efficiently entrap the non-toxic PFC gas at physiological temperature and perform as good acoustic enhancers over a wide frequency range and out of resonant conditions, as tested in both *in vitro* and *in vivo* experiments. The peculiar structural stability of NBs, with respect to recently developed nano-sized bubbles[39] ensures a durable acoustic efficiency, as the presence of the closed amphiphilic shell appears to constitute a good structural barrier against collapse or gas diffusion and leakage, usually experienced by nanobubbles, thus improving the persistence of US contrast in diagnostics. The time stability of their formulation in the form of aqueous dispersions distinguishes these NBs as compared to current marketed products, which are lyophilized and dehydrated to be stored, and then need to be reconstituted before use. Of note, the possibility to co-load hydrophilic and lipophilic therapeutic and/or diagnostic agents in the multilayered amphiphilic envelope of NBs, without depleting their US performance, illustrates their potential as a platform for the

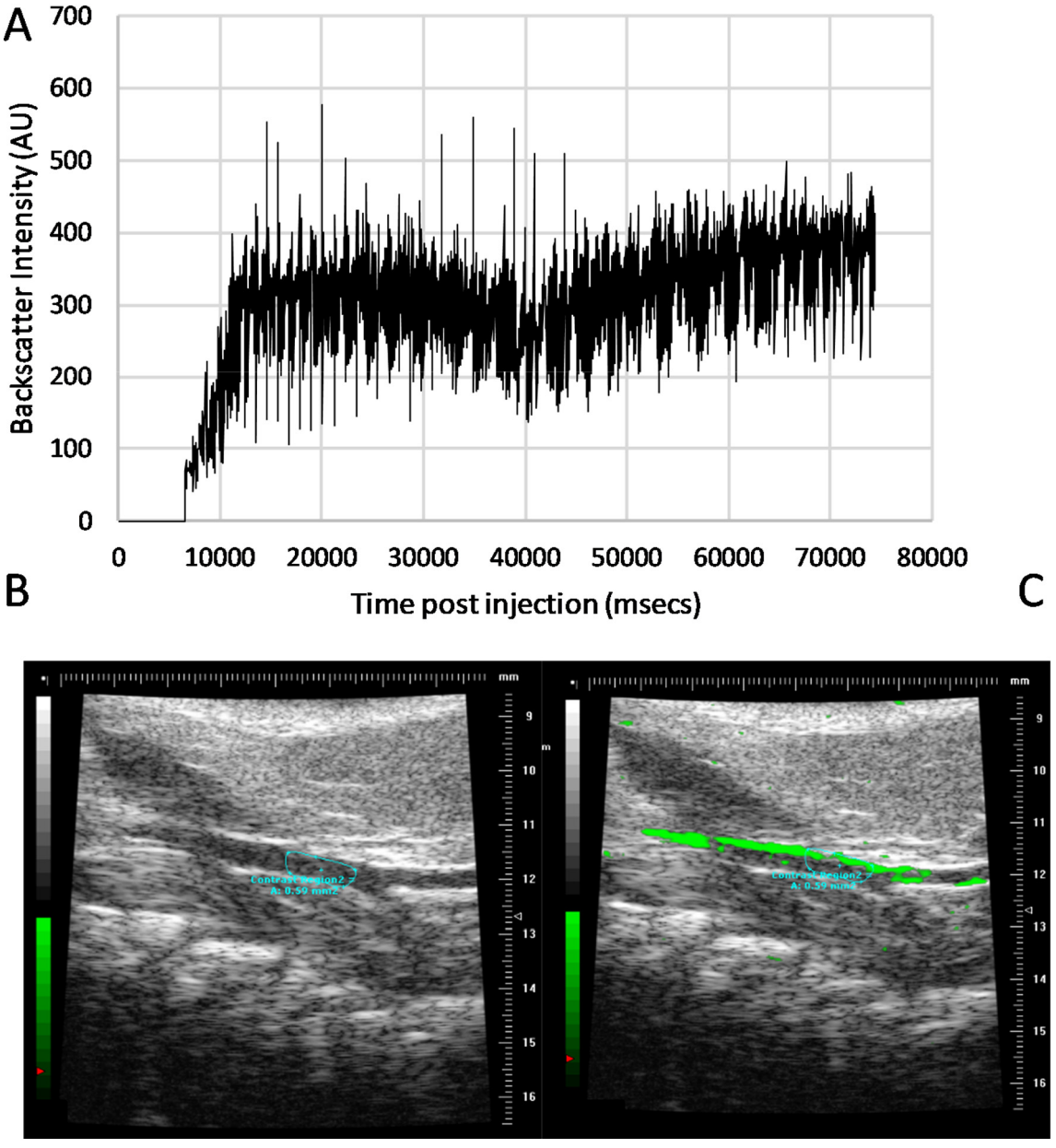

Fig. 7. A) Backscatter enhancement relative to mean reference baseline measurements, measured in carotid artery before, during and after a contrast injection of 50 μl of Span-20 nanobubbles. B) Baseline image of mouse carotid artery showing region-of-interest, outlined in blue. C) Contrast-enhanced image with green showing presence of contrast. Images acquired at 30 MHz using a Vevo 770 preclinical ultrasound scanner.

design and production of versatile carriers to be used in US-assisted diagnostic, therapeutic and theranostic applications.

Abbreviations

FDA	Food and Drug Administration
US	ultrasound
MBs	microbubbles
NBs	nanobubbles

Supplementary data to this article can be found online at https://doi.org/10.1016/j.nano.2022.102611.

CRediT authorship contribution statement

Patrizia N Hanieh, Caterina Ricci, Federica Rinaldi, Elena Del Favero, Carlotta Marianecci: Conceptualization, Investigation, Writing - original draft preparation, Andrea Bettucci, Laura Cantù: Investigation, Data curation, Writing - original draft preparation. Roberto Marotta: Investigation. Carmel M Moran: Data curation, Supervision. Maria Carafa: Conceptualization. All authors: Writing - reviewing and editing.

Declaration of competing interest

The authors declare the following competing financial interest(s): the authors Federica Rinaldi, Carlotta Marianecci, Maria Carafa and Andrea Bettucci are inventors of a patent on the nanobubbles used in the present research. The other co-authors have no conflict of interest.

Acknowledgment

We thank ESRF and ID02 staff for beamtime and assistance (10.15151/ESRF-ES-281427365). E.D.F. thanks BIOMETRA Dept. for partial support (PSR2020_DEL_FAVERO).

References

1. Feinstein SB, Shah PM, Bing RJ, Meerbaum S, Corday E, Chang B-L, et al. Microbubble dynamics visualized in the intact capillary circulation. *J Am Coll Cardiol* 1984;**4**(3):595-600.
2. Frinking P, Segers T, Luan Y, Tranquart F. Three decades of ultrasound contrast agents: a review of the past, present and future improvements. *Ultrasound Med Biol* 2020;**46**(4):892-908.
3. Sun C, Sboros V, Butler MB, Moran CM. In vitro acoustic characterization of three phospholipid ultrasound contrast agents from 12 to 43 MHz. *Ultrasound Med Biol* 2014;**40**(3):541-50.
4. Lee JY, Minami Y, Choi BI, Lee WJ, Chou Y-H, Jeong WK, et al. The AFSUMB consensus statements and recommendations for the clinical practice of contrast-enhanced ultrasound using sonazoid. *J Med Ultrasound* 2020;**28**(2):59.
5. Dietrich CF, Nolsøe CP, Barr RG, Berzigotti A, Burns PN, Cantisani V, et al. Guidelines and good clinical practice recommendations for contrast enhanced ultrasound (CEUS) in the liver–update 2020–WFUMB in cooperation with EFSUMB, AFSUMB, AIUM, and FLAUS. *Ultraschall in der Medizin* 2020;**41**(05):562-85.
6. Zlitni A, Gambhir SS. Molecular imaging agents for ultrasound. *Curr Opin Chem Biol* 2018;**45**:113-20.
7. Kooiman K, Roovers S, Langeveld SA, Kleven RT, Dewitte H, O'Reilly MA, et al. Ultrasound-responsive cavitation nuclei for therapy and drug delivery. *Ultrasound Med Biol* 2020;**46**(6):1296-325.
8. Ingram N, McVeigh LE, Abou-Saleh RH, Maynard J, Peyman SA, McLaughlan JR, et al. Ultrasound-triggered therapeutic microbubbles enhance the efficacy of cytotoxic drugs by increasing circulation and tumor drug accumulation and limiting bioavailability and toxicity in normal tissues. *Theranostics* 2020;**10**(24):10973.
9. Logan K, Foglietta F, Nesbitt H, Sheng Y, McKaig T, Kamila S, et al. Targeted chemo-sonodynamic therapy treatment of breast tumours using ultrasound responsive microbubbles loaded with paclitaxel, doxorubicin and Rose Bengal. *Eur J Pharm Biopharm* 2019;**139**:224-31.
10. Nesbitt H, Sheng Y, Kamila S, Logan K, Thomas K, Callan B, et al. Gemcitabine loaded microbubbles for targeted chemo-sonodynamic therapy of pancreatic cancer. *J Control Release* 2018;**279**:8-16.
11. Wu H, Abenojar EC, Perera R, An T, Exner AA. Time-intensity-curve analysis and tumor extravasation of nanobubble ultrasound contrast agents. *Ultrasound Med Biol* 2019;**45**(9):2502-14.
12. Fang J, Nakamura H, Maeda H. The EPR effect: unique features of tumor blood vessels for drug delivery, factors involved, and limitations and augmentation of the effect. *Adv Drug Deliv Rev* 2011;**63**(3):136-51.
13. Jadhav AJ, Barigou M. Bulk nanobubbles or not nanobubbles: that is the question. *Langmuir* 2020;**36**(7):1699-708.
14. Omata D, Maruyama T, Unga J, Hagiwara F, Munakata L, Kageyama S, et al. Effects of encapsulated gas on stability of lipid-based microbubbles and ultrasound-triggered drug delivery. *J Control Release* 2019;**311**:65-73.
15. Lin C-Y, Pitt WG. Acoustic droplet vaporization in biology and medicine. *Biomed Res Int* 2013;**2013**.
16. Li DS, Schneewind S, Bruce M, Khaing Z, O'Donnell M, Pozzo L. Spontaneous nucleation of stable perfluorocarbon emulsions for ultrasound contrast agents. *Nano Lett* 2018;**19**(1):173-81.
17. Batchelor DV, Armistead FJ, Ingram N, Peyman SA, Mclaughlan JR, Coletta PL, et al. Nanobubbles for therapeutic delivery: production, stability and current prospects. *Curr Opin Colloid Interface Sci* 2021;**54**101456.
18. Perera R, Hernandez C, Cooley M, Jung O, Jeganathan S, Abenojar E, et al. Contrast enhanced ultrasound imaging by nature-inspired ultrastable echogenic nanobubbles. *Nanoscale* 2019;**11**(33):15647-58.
19. Eklund F, Alheshibri M, Swenson J. Differentiating bulk nanobubbles from nanodroplets and nanoparticles. *Curr Opin Colloid Interface Sci* 2021;**53**101427.
20. Beltramo PJ, Gupta M, Alicke A, Liascukiene I, Gunes DZ, Baroud CN, et al. Arresting dissolution by interfacial rheology design. *Proc Natl Acad Sci* 2017;**114**(39):10373-8.
21. Taccoen N, Lequeux F, Gunes DZ, Baroud CN. Probing the mechanical strength of an armored bubble and its implication to particle-stabilized foams. *Phys Rev X* 2016;**6**(1)011010.
22. Batchelor DV, Abou-Saleh RH, Coletta PL, McLaughlan JR, Peyman SA, Evans SD. Nested nanobubbles for ultrasound-triggered drug release. *ACS Appl Mater Interfaces* 2020;**12**(26):29085-93.
23. Hernandez C, Nieves L, de Leon AC, Advincula R, Exner AA. Role of surface tension in gas nanobubble stability under ultrasound. *ACS Appl Mater Interfaces* 2018;**10**(12):9949-56.
24. Schutt EG, Klein DH, Mattrey RM, Riess JG. Injectable microbubbles as contrast agents for diagnostic ultrasound imaging: the key role of perfluorochemicals. *Angew Chem Int Ed* 2003;**42**(28):3218-35.
25. Kremer JR, Mastronarde DN, McIntosh JR. Computer visualization of three-dimensional image data using IMOD. *J Struct Biol* 1996;**116**(1):71-6.
26. Doucet M, Cho J, Alina G, Bakker J, Bouwman W, Butler P, et al. *SasView Version 4.2. 2*; 2019.
27. Lentz BR. Membrane "fluidity" as detected by diphenylhexatriene probes. *Chem Phys Lipids* 1989;**50**(3–4):171-90.
28. Alippi A, Bettucci A, Biagioni A, D'Orazio A, Germano M, Passeri D. Photoacoustic cell for ultrasound contrast agent characterization. *Rev Sci Instrum* 2010;**81**(10)104903.
29. Xu J, Salari A, Wang Y, He X, Kerr L, Darbandi A, et al. Microfluidic generation of monodisperse nanobubbles by selective gas dissolution. *Small* 2021;**17**(20):2100345.
30. Zhang J, Chen Y, Deng C, Zhang L, Sun Z, Wang J, et al. The optimized fabrication of a novel nanobubble for tumor imaging. *Front Pharmacol* 2019;**10**:610.
31. Han D, Zhang B, Dong J, Yang B, Peng Y, Wang J, et al. 1, 2-Dimyristoyl-sn-glycero-3-phosphocholine promotes the adhesion of nanoparticles to bio-membranes and transport in rat brain. *RSC Adv* 2021;**11**(56):35455-62.
32. Pardakhty A, Shakibaie M, Daneshvar H, Khamesipour A, Mohammadi-Khorsand T, Forootanfar H. Preparation and evaluation of niosomes containing autoclaved leishmania major: a preliminary study. *J Microencapsul* 2012;**29**(3):219-24.
33. Marianecci C, Di Marzio L, Rinaldi F, Celia C, Paolino D, Alhaique F, et al. Niosomes from 80s to present: the state of the art. *Adv Colloid Interface Sci* 2014;**205**:187-206.
34. Rinaldi F, Hanieh PN, Imbriano A, Passeri D, Del Favero E, Rossi M, et al. Different instrumental approaches to understand the chitosan coated niosomes/mucin interaction. *J Drug Deliv Sci Technol* 2020;**55**101339.
35. The resonance frequency of sonovue/spl trade/as observed by high-speed optical imaging. In: Van der Meer S, Versluis M, Lohse D, Chin C, Bouakaz A, De Jong N, editors. *IEEE Ultrasonics Symposium*. IEEE; 2004. 2004.

36. Zemb T, Lindner P. Neutron, X-rays and light. *Scattering Methods Applied to Soft Condensed Matter*; 2002. North Holland.
37. Rinaldi F, del Favero E, Moeller J, Hanieh PN, Passeri D, Rossi M, et al. Hydrophilic silver nanoparticles loaded into niosomes: physical–chemical characterization in view of biological applications. *Nanomaterials* 2019;**9**(8): 1177.
38. Marianecci C, Di Marzio L, Del Favero E, Cantù L, Brocca P, Rondelli V, et al. Niosomes as drug nanovectors: multiscale pH-dependent structural response. *Langmuir* 2016;**32**(5):1241-9.
39. Zhou L, Wang S, Zhang L, Hu J. Generation and stability of bulk nanobubbles: a review and perspective. *Curr Opin Colloid Interface Sci* 2021;**53**101439.